Received: 5 September 2024 | Revised: 28 October 2024 | Accepted: 24 February 2025 | Published online: 20 March 2025

RESEARCH ARTICLE

Journal of Optics and Photonics Research
2025, Vol. 3(1) 1–10
DOI: 10.47852/bonviewJOPR52024257

BON VIEW PUBLISHING

Quasiparticle-Photon Transitions in Superconductors Within a QED Cavity

Jayanti Chand[1], Kishori Yadav[1] and Saddam Husain Dhobi[2,*]

[1]*Department of Physics, Tribhuvan University (Patan Multiple Campus), Nepal*

[2]*Central Department of Physics, Tribhuvan University, Nepal*

Abstract: Quasiparticle-photon interactions in superconductors within a quantum electrodynamics (QED) cavity are crucial for quantum technologies and superconducting circuits. These transitions, driven by confined electromagnetic fields, influence quasiparticle dynamics and superconducting properties, enabling novel quantum states and hybrid quantum systems. This study investigates the transition rates for photon-quasiparticle emission from a cavity, using mathematical and numerical analysis methods. The transition rate function $F(E)$ was evaluated for different values of normalized superconductor quasiparticle density states (n), specifically $n = 1$ and $n = 10$, across an energy gap range from −2 eV to 2 eV. The analysis reveals that for $n = 1$, the transition rate exhibits a pronounced peak near the Fermi energy, indicating higher transition probabilities at lower values of n due to fewer available states. Conversely, for $n = 10$, the transition rate profile becomes broader and the peak height diminishes, reflecting an increased number of states and a more dispersed transition rate. Additionally, the inverse temperature β shows an inverse relationship with the transition rate $F(E)$, where higher temperatures (lower β) lead to increased transition rates due to enhanced thermal excitation. The study also examines the effective temperature T_{QCR} of the quantum cavity resonator (QCR) environment as a function of the energy gap and photon frequency, showing that T_{QCR} generally increases with the magnitude of the energy gap and decreases with increasing photon frequency. The scientific significance of these studies lies in their contribution to understanding the complex dynamics of photon-quasiparticle transitions, particularly how transition rates vary with energy gaps, photon frequencies, and temperature. This insight is crucial for improving coherence times and minimizing decoherence in superconducting quantum circuits. The potential application value is significant for advancing quantum computing and communication, as optimizing transition rates can lead to more efficient qubit initialization, readout, and control, ultimately enhancing the performance and scalability of quantum technologies.

Keywords: photon emission, quasiparticle emission, transition rates, energy gap, cavity dynamics, thermal excitation, effective temperature

1. Introduction

Quasiparticle-photon transitions in superconductors are critical to the operation of superconducting quantum circuits, which form the foundation for advanced quantum technologies such as quantum computing and quantum communication. These transitions occur when quasiparticles—electron-like excitations in a superconductor—interact with photons confined in a quantum electrodynamics (QED) cavity. The controlled environment of a QED cavity allows for precise manipulation and observation of these interactions, making it an ideal platform for studying fundamental quantum phenomena. In circuit quantum electrodynamics (cQED), a superconducting microwave resonator is coupled to a quantum circuit, facilitating the exchange of energy between the electromagnetic field and the superconducting circuit. This interaction is essential for tasks such as qubit initialization, readout, and reset. However, quasiparticles can cause decoherence and energy loss in the system, posing significant challenges to achieving long coherence times and high-fidelity operations in quantum devices. The thermal distribution within the resonator was measured using instruments capable of detecting temperatures down to 60 mK. The superconducting microwave resonator's thermal state and its coupling to external baths were monitored with precision equipment, ensuring accurate data collection [1]. The initial thermal state of the resonator was established by heating the attenuator using a detuned heater signal. This process increased the resonator population, setting up strong spectral lines required for the experiment. The thermal state of the resonator, characterized by a temperature above 300 mK, was gradually decreased to approximately 100 mK using the QCR, effectively refrigerating the resonator. The relationship between the QCR and the thermal states was explored by examining the influence of the QCR on the electromagnetic environment's effective temperature. The mean photon number $n_{thermal} = \frac{1}{\left\{exp\left[\frac{\hbar\omega_r}{k_B T}\right]+1\right\}}$ was calculated using the Bose occupation number [2]. where $\hbar$ is the reduced Planck constant, ω_r is the resonator frequency, k_B is the Boltzmann constant, and T_{QRC} is the temperature.

Tabatabaei and Jahangiri [3] present a semiclassical theory describing heat transfer in quantum dot junctions capacitively coupled to a resonator, focusing on electron tunneling processes that can cool or heat the system and influence photon absorption

*Corresponding author: Saddam Husain Dhobi, Central Department of Physics, Tribhuvan University, Nepal. Email: saddam@ran.edu.np

and emission. Krasnok et al. [4] review advancements in superconducting microwave cavities, essential for scalable quantum systems, and highlight challenges in achieving longer coherence times in qubits. Connolly et al. [5] explore energy distribution in out-of-equilibrium quasiparticles in transmon qubits, demonstrating how gap asymmetry can manipulate parity. Cheng et al. [6] analyze transient current dynamics in superconductor-quantum dot junctions, identifying distinct oscillatory behaviors when bias is turned off or on. Dubovitskii et al. [7] discuss quasiparticle-induced decoherence in Schrödinger cat qubits, highlighting the effect of quasiparticles in nonequilibrium conditions. Finally, Pita-Vidal et al. [8] demonstrate strong, tunable supercurrent-mediated coupling between distant Andreev spin qubits, offering potential for efficient two-qubit gates. Krasnok et al. [4] examine the progress made in superconducting microwave cavities with ultra-high Q-factors, which are essential for quantum computing. Their study covers enhancements in coherence times, challenges posed by noise and damping, and advancements in 3D qubits and multi-qubit systems. The authors also highlight the potential for new materials and error correction methods. Superconducting quantum circuits [9] have emerged as a key platform for developing quantum information systems [10, 11]. These devices leverage insights from open quantum systems and can benefit from reservoir engineering [12]. The versatility of QCR allows it to serve as a tunable dissipation source for quantum-electric devices [13–15], with applications ranging from qubit reset [16] to fundamental physics phenomena like Lamb shifts [17].

QED has emerged as a crucial framework for understanding the interaction between light (photons) and matter (electrons), particularly in superconducting circuits. This research delves into cQED, which explores the coupling of quantum circuits with microwave resonators. The development of cQED has significantly advanced our ability to manipulate quantum systems, enabling progress in quantum information processing, quantum communication, and quantum metrology [9]. In practical applications, the quantum state of the circuit is manipulated using a series of microwave pulses that drive transitions between states, followed by a measurement pulse to probe the cavity. Typically, a low-power probe is used to minimize back-action on the system, though this approach suffers from a low signal-to-noise ratio, leading to incomplete state discrimination. This "weak measurement" regime has been extensively studied, offering insights into measurement projection and enabling the application of real-time feedback on the system [18].

QED explores atom-photon interactions in cavities, building on Purcell's 1946 work showing resonators enhance spontaneous emission. Modern cavity QED focuses on quantum coherence and decoherence control, essential for quantum computation [19]. In astronomy, low-temperature detectors like microwave kinetic inductance detectors enable powerful arrays for challenging observations [20]. bhnSilicon nitride microring cavities can efficiently couple intrinsic emitters to whispering gallery modes for quantum photonic applications [21]. Quantum superpositions, vital for quantum computing, have been created in resonators using phase qubits and Wigner tomography [22]. Hybrid photonic platforms offer solutions for quantum information, combining technologies for quantum teleportation and large-scale devices [23].

In contrast, our focus is on the strong measurement regime, where the increased measurement power allows for unambiguous state discrimination. However, this regime is not without challenges. As the measurement power increases, the nonlinearity of the system becomes apparent, particularly the influence of the number of photons in the cavity on the system's dynamics [24]. The role of photon numbers in cQED has been theoretically explored, especially in systems where a pure two-level qubit is coupled to a harmonic oscillator. Key effects include changes in the state-dependent cavity frequency shift and alterations in the qubit's dynamics, such as relaxation and excitation rates [25]. These effects are especially pronounced in quantum circuits with low anharmonicity, where the two-level approximation fails at high power levels [26].

In this work, we experimentally investigate these effects using a highly anharmonic quantum circuit—an atomic-scale weak link in a superconducting loop [27]. This weak link, known as an atomic contact, contains a few spin-degenerate Andreev levels within the superconducting gap [28]. We conducted continuous measurements of the cavity at various microwave powers, analyzed the state discrimination, and extracted the transition rates across multiple contact configurations with different Andreev level energies. The purpose of this research is to explore how QCR can be employed to regulate the thermal state of a superconducting resonator and to quantify the impact of this regulation on the system's photon population and overall performance. This study aims to fill the knowledge gap regarding the thermal dynamics of quantum circuits and provide practical solutions to enhance system coherence and stability under varying thermal conditions. Moreover, this work investigates how precise control of the system's effective temperature can mitigate issues related to thermal population and quasiparticle-induced decoherence [29], thereby contributing to the ongoing efforts to scale up quantum computing systems. While significant progress has been made in understanding photon-quasiparticle transitions within superconducting quantum circuits, existing studies primarily focus on the weak measurement regime, where the signal-to-noise ratio is low and state discrimination is incomplete. The dynamics of photon-quasiparticle transitions under strong measurement conditions, where the number of photons in the cavity plays a critical role, remain less explored. Additionally, the influence of energy gap variations and photon frequency on the effective temperature of the QCR environment has not been thoroughly investigated. This leaves a gap in understanding how these factors affect transition rates, especially under different thermal conditions. The motivation behind this research is to better understand the role of quasiparticle-photon transitions in superconducting circuits, particularly how they influence the thermal states and coherence properties of the system. By exploring the impact of thermal fluctuations and external control mechanisms, such as QCR, this work aims to mitigate quasiparticle-induced losses and optimize the performance of superconducting qubits. The study addresses key challenges in achieving robust quantum control by examining the relationship between quasiparticle dynamics and photon interactions within a controlled QED environment. Parasitic two-level system defects limiting superconducting qubit coherence have been characterized using strong qubit drive techniques, and advancements in epitaxial materials and experimental techniques aim to enable precise studies of QED phenomena, including noise models and qubit-defect interactions [30, 31].

The necessity of this study is underscored by the limited exploration of photon-quasiparticle transitions under strong measurement conditions, as highlighted in existing literature. While substantial research has been done on weak measurement regimes, where the signal-to-noise ratio is low and state discrimination remains incomplete, the dynamics of strong measurement regimes, where photon numbers critically influence

system behavior, are still rarely investigated [24, 26]. Furthermore, the effects of energy bandgap variations and photon frequencies on the effective temperature of the QCR environment are not well understood, leaving a knowledge gap in how these factors impact transition rates across different thermal conditions. Addressing this gap, as noted by Krasnok et al. [4] and Connolly et al. [5], is essential for advancing our understanding of quasiparticle-photon interactions and improving the coherence and stability of quantum systems. By filling this void, the study aims to optimize quantum circuit performance, especially in achieving scalable quantum technologies.

2. Materials and Methods

The research was conducted using a QED cavity integrated with a superconducting microwave resonator. The cavity was designed to facilitate the interaction between quasiparticles and photons under varying thermal conditions. A QCR was employed to manage the thermal states of the electromagnetic environment within the cavity. The QCR operates by controlling the effective temperature T_{QCR} of the system, thereby influencing the mean photon number as described by the Bose occupation number. An attenuator was used to emit black-body radiation into the resonator, creating an initial thermal state with strong spectral lines for clear signal acquisition. A detuned heater signal was utilized to adjust the temperature of the attenuator, thereby controlling the thermal population of the resonator. The thermal distribution within the resonator was measured using instruments capable of detecting temperatures down to 60 mK. The sketch of QED cavity system is represented in Figure 1 [32, 33] below.

The superconducting microwave resonator's thermal state and its coupling to external baths were monitored with precision equipment, ensuring accurate data collection. The initial thermal state of the resonator was established by heating the attenuator using a detuned heater signal. This process increased the resonator population, setting up strong spectral lines required for the experiment. The thermal state of the resonator, characterized by a temperature above 300 mK, was gradually decreased to approximately 100 mK using the QCR, effectively refrigerating the resonator. The relationship between the QCR and the thermal states was explored by examining the influence of the QCR on the electromagnetic environment's effective temperature. The mean photon number $n_{thermal} = \frac{1}{\left\{exp\left[\frac{\hbar\omega_r}{k_B T}\right]+1\right\}}$ was calculated using the Bose occupation number [2]. where $\hbar$ is the reduced Planck constant, ω_r is the resonator frequency, k_B is the Boltzmann constant, and T_{QRC} is the temperature.

Figure 1

Representative experimental setup for cavity quantum electrodynamics. (A) In microwave cavity QED experiments, atoms in a thermal beam (O) are prepared in Rydberg states, (B) before passing through a superconducting cavity, (C) interrogation of intracavity dynamics is performed by state-selective detection of atoms via field ionization, and (D) the intracavity atoms can be driven by a microwave source (S) for direct state manipulation

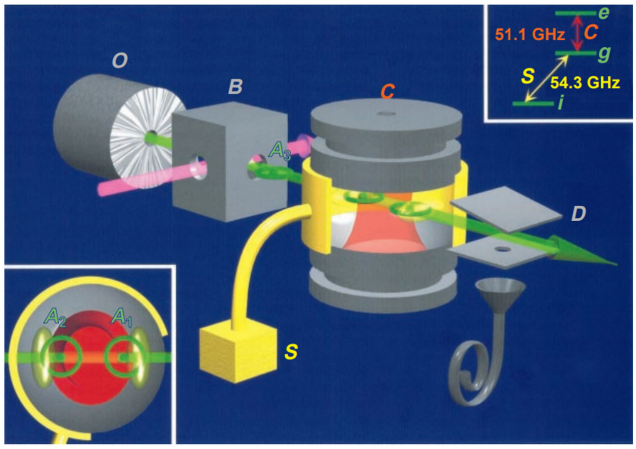

$$T_{QCR} = \frac{\hbar\omega_r}{k_B}\left[\ln\left(\frac{F(eV + \hbar\omega_r)}{F(eV - \hbar\omega_r)}\right)\right]^{-1} \quad (1)$$

This Equation (1) describes the effective temperature T_{QCR} of a QCR that couples to a superconducting microwave resonator. This effective temperature is a key parameter in understanding the refrigeration effect, which involves the cooling of the resonator via quasiparticle tunneling processes within a QED cavity. The function $F(E)$ represents the normalized rate of forward quasiparticle tunneling and is given by the integral derived by Karimi et al. [34] and defined as:

$$F(E) = \frac{1}{h}\int d\varepsilon\, n_s(\varepsilon)[1 - f_s(\varepsilon)]f_N(\varepsilon - E) \quad (2)$$

In this Equation (2), h is Planck's constant, $n_s(\varepsilon)$ is the normalized superconductor quasiparticle density of states, $f_s(\varepsilon)$ is the Fermi-Dirac distribution function for the superconducting lead, $f_N(\varepsilon - E)$ is the Fermi-Dirac distribution function for the normal-metal lead. The term $n_s(\varepsilon)$ represents the density of quasiparticle states in the superconductor, which is influenced by the superconducting gap Δ. The density of states $n_s(\varepsilon)$ becomes significant when ε is close to the superconducting gap [35], where quasiparticles start to appear. The Fermi-Dirac distribution functions $f_s(\varepsilon)$ and $f_N(\varepsilon - E)$ describe the occupation probability of energy states in the superconductor and the normal metal, respectively. The expression $[1 - f_s(\varepsilon)]$ ensures that only unoccupied states in the superconductor contribute to the tunneling process. The effective temperature T_{QCR} is obtained by considering the balance between the rates of forward and backward quasiparticle tunneling processes. The forward process is represented by $F(\text{eV} + \hbar\omega_r)$, where the energy bias $E = \text{eV} + \hbar\omega_r$ includes the energy of the resonator's photon $\hbar\omega_r$. The backward process is represented by $F(\text{eV}-\hbar\omega_r)$, where the photon energy reduces the effective energy bias.

$$n_s(\varepsilon) = \left|Re\left\{\frac{\varepsilon + i\gamma_D\Delta}{\sqrt{(\varepsilon + i\gamma_D\Delta)^2 - \Delta^2}}\right\}\right| \quad (3)$$

This expression accounts for the broadening of quasiparticle states due to a finite lifetime, characterized by γ_D, which leads to a complex energy term $\varepsilon + i\gamma_D\Delta$. The density of states is crucial for determining the rate at which quasiparticles can tunnel, directly affecting the cooling power of the QCR. In simpler terms, γ_D indicates how long a quasiparticle can exist before decaying, and this decay shortens the coherence of the quasiparticle. The larger γ_D is, the more smeared the quasiparticle density of states $n_s(\varepsilon)$ becomes, affecting how efficiently quasiparticles can tunnel between the superconductor and the normal metal. This tunneling rate, in turn, impacts the cooling performance of the QCR as it governs how well energy (in the form of heat) is transferred out of the system. Thus, γ_D is essential for

understanding the practical limitations of quasiparticle tunneling and the refrigeration effect within superconducting quantum systems. In this Equation (3), $n_s(\varepsilon)$ represents the normalized superconducting quasiparticle density of states inside the cavity, which significantly influences the photon-quasiparticle transition rate. The density of states reflects the number of available quasiparticle states at a given energy level, and its normalization accounts for variations in the system's parameters, such as temperature or energy gap. A lower n value, indicating fewer available quasiparticle states, leads to a more concentrated transition rate near the Fermi energy, as fewer states are available for energy exchange. Conversely, a higher n broadens the transition rate profile, reflecting more states available for transitions, thereby distributing the energy transfer over a wider range of energies. The normalized quasiparticle density of states serves as a critical optimizing parameter because it governs how efficiently energy is transferred between the photons and quasiparticles, ultimately impacting the overall performance of the superconducting quantum system. Since we are considering the case of both photons and quasiparticle transmittance across the cavity so modification of Equation (2) is needed and for this we have $f_s(\varepsilon) = \frac{1}{1+e^{\beta\left(\varepsilon - E_f\right)}}$ and $f_N(\varepsilon - E) = \frac{1}{1+e^{\beta\left(\varepsilon - E - E_f\right)}}$, and hence from these distribution functions and Equation (3), Equation (2) becomes:

$$F(E) = \frac{1}{h}\int d\varepsilon \left| Re\left\{\frac{\varepsilon + i\gamma_D\Delta}{\sqrt{(\varepsilon + i\gamma_D\Delta)^2 - \Delta^2}}\right\}\right| \left[1 - \frac{1}{1 + e^{\beta\left(\varepsilon - E_f\right)}}\right]\frac{1}{1 + e^{\beta\left(\varepsilon - E - E_f\right)}} \tag{4}$$

This modified equation for $F(E)$ includes the effects of both photon and quasiparticle interactions. The main modification comes from the presence of the complex energy term $\varepsilon + i\gamma_D\Delta$, where γ_D represents a damping factor associated with the quasiparticle lifetime. The term $Re\left\{\frac{\varepsilon + i\gamma_D\Delta}{\sqrt{(\varepsilon + i\gamma_D\Delta)^2 - \Delta^2}}\right\}$ represents the real part of the Green's function, which accounts for the quasiparticle dynamics within the superconducting state. It captures the influence of the superconducting gap and the damping factor γ_D on the quasiparticle states. The integral now accounts for the complex interaction between the quasiparticles and photons, with the damping factor γ_D indicating how the quasiparticle states are affected by inelastic processes. This is essential for modeling the realistic behavior of quasiparticles in a superconducting cavity. One obtains the dependence of the cavity pull on n, the number of photons in the cavity $\chi(n) \approx \chi_0(1 - 2\lambda^2 n) = \chi_0\left(1 - \frac{n}{2n_{crit}}\right)$, with $n_{crit} = (\Delta/2g)^2$ the critical photon number. This expression was extended to arbitrary ratio $n/2n_{crit}$ by exact diagonalization, yielding $\chi(n) = \frac{\chi_0}{\sqrt{1 + n/n_{crit}}}$ and hence, transition of photon and quasiparticle from cavity is obtained as:

$$F(E) = \frac{1}{h}\int d\varepsilon \left| Re\left\{\frac{\varepsilon + i\gamma_D\Delta}{\sqrt{(\varepsilon + i\gamma_D\Delta)^2 - \Delta^2}}\right\}\right| \left[1 - \frac{1}{1 + e^{\beta\left(\varepsilon - E_f\right)}}\right]\frac{n}{1 + e^{\beta\left(\varepsilon - E - E_f\right)}} \tag{5}$$

Here, the photon number n is directly included in the expression for $F(E)$. The presence of n reflects how the tunneling rate is influenced by the number of photons in the cavity, which can enhance or suppress the quasiparticle tunneling depending on the photon density. Substituting the value of n we get $\frac{A_0^2}{4(\delta \pm \chi(n))^2 + k^2} = n$, we have:

$$F(E) = \frac{1}{h}\int d\varepsilon \left| Re\left\{\frac{\varepsilon + i\gamma_D\Delta}{\sqrt{(\varepsilon + i\gamma_D\Delta)^2 - \Delta^2}}\right\}\right| \left[1 - \frac{1}{1 + e^{\beta\left(\varepsilon - E_f\right)}}\right]\frac{1}{1 + e^{\beta\left(\varepsilon - E - E_f\right)}}\frac{A_0^2}{4(\delta \pm \chi(n))^2 + k^2} \tag{6}$$

The novelty of the developed Equation (6) lies in its integration of both photon and quasiparticle dynamics within a cavity, marking a significant extension beyond previous studies that focused solely on quasiparticle transitions. By incorporating the energy shifts due to photons ($\pm\hbar\omega_r$) into the tunneling rates, the equation captures how photon-quasiparticle interactions affect the energy landscape and dynamics within the system. This theoretical model reveals the influence of photon energy on quasiparticle tunneling, illustrating the dual role of photons in either facilitating or hindering tunneling based on energy bias shifts. Furthermore, the model allows the exploration of temperature-dependent effects on photon and quasiparticle interactions, offering a more comprehensive understanding of the coupled dynamics in a cavity, an aspect previously unaddressed in standard quasiparticle-only transition studies. This represents a novel advancement in understanding photon-quasiparticle transitions in cavity systems. Also, we have $F(eV + \hbar\omega_r) = \frac{1}{h}\int d\varepsilon\, n_s(\varepsilon)\ [1 - f_s(\varepsilon)]f_N\ (\varepsilon - eV - \hbar\omega_r)$ and $F(eV - \hbar\omega_r) = \frac{1}{h}\int d\varepsilon\, n_s(\varepsilon)[1 - f_s(\varepsilon)]\ f_N(\varepsilon - eV + \hbar\omega_r)$ where $f_N(\varepsilon - E) = \frac{1}{1+e^{\frac{\varepsilon - E - E_f}{k_B T}}} = \frac{1}{1+e^{\beta\left(\varepsilon - E - E_f\right)}}$ than

$$f_N(\varepsilon - eV + \hbar\omega_r) = \frac{1}{1 + e^{\beta(\varepsilon - eV + \hbar\omega_r - E_f)}} \tag{7}$$

$$f_N(\varepsilon - eV - \hbar\omega_r) = \frac{1}{1 + e^{\beta(\varepsilon - eV - \hbar\omega_r - E_f)}} \tag{8}$$

These expressions represent the tunneling rates when the energy bias is shifted by $\pm\hbar\omega_r$, which corresponds to the energy of the photons in the cavity. $F(eV + \hbar\omega_r)$ and $F(eV - \hbar\omega_r)$, these rates indicate how the presence of photons alters the energy landscape for quasiparticle tunneling, thereby affecting the overall dynamics of the system. The energy shifts $\hbar\omega_r$ signify how the photon energy is involved in the quasiparticle tunneling process, either assisting or hindering the tunneling depending on the direction of the energy shift. Also, from Equation (1) we can obtain temperature nature with photons and quasiparticles.

3. Results and Discussion

3.1. Transition rates for photon and quasiparticle emission

The transition of photons and quasiparticles from the cavity was analyzed using the expression given in Equation (5). The numerical evaluation of the transition rate function $F(E)$ was performed for different parameter. The results of these calculations are plotted as functions of the energy gap E. The expression for $F(E)$ incorporates the complex interplay between photon and quasiparticle dynamics within the cavity. This relationship is governed by factors such as the inverse temperature (β), the Fermi energy (E_f), and the parameters γ_D and Δ which represent dissipation and the characteristic energy

Figure 2
Transition rate with energy gap for photon-quasiparticle density of states (a) $n = 1$ and (b) $n = 10$

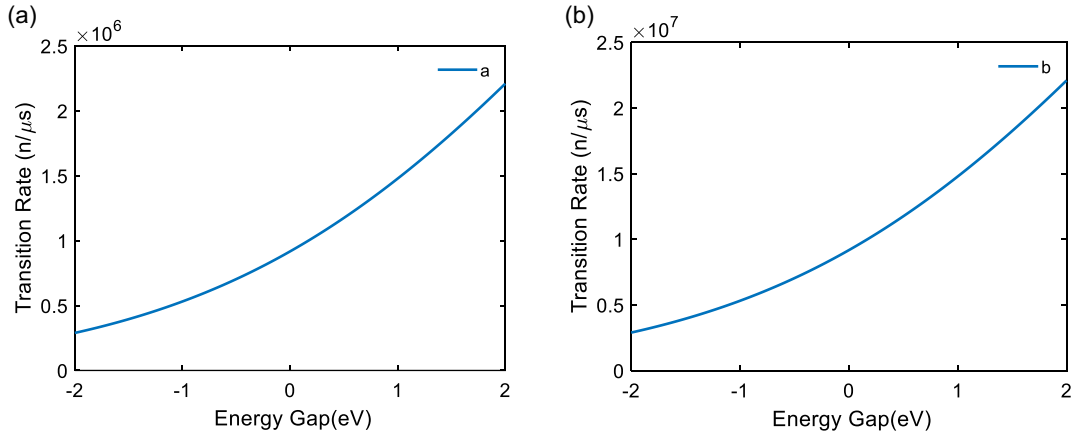

scale, respectively. The integrand also involves a Fermi-Dirac distribution, reflecting the quantum statistics of the system. For $n = 1$, the transition rate $F(E)$ was computed across the energy gap range from -2 eV to 2 eV. The resulting curve is shown in Figure 2(a). The function $F(E)$ exhibits a peak near the Fermi energy, indicating a higher probability of transitions occurring when the energy gap is close to the Fermi level. This behavior aligns with the expectation that at lower values of n, the system has fewer available states for transitions, leading to a sharper and more localized peak in the transition rate. For $n = 10$, the transition rate $F(E)$ was similarly evaluated, and the results are shown in Figure 2(b). Compared to the case of $n = 1$, the transition rate profile for $n = 10$ is broader and exhibits a reduced peak height. This broader distribution indicates that as n increases, the system's available states for transitions also increase, leading to a more dispersed transition rate over the energy gap range. The lower peak suggests that individual transition probabilities decrease as the number of available states increases, diluting the overall transition likelihood at specific energy gaps.

The results demonstrate how the transition rates from the cavity depend on the energy gap and the parameter n, which could represent the number of particles or states in the system. For lower n, the system shows a pronounced peak in transition rates near the Fermi energy, indicating more localized and probable transitions. As n increases, the transition rates become more spread out, reflecting a greater distribution of states available for transitions, which leads to a broader but less intense peak. These findings provide insights into the photon and quasiparticle dynamics within the cavity, with potential implications for understanding energy transfer processes in quantum systems. The variation in transition rates with n could be relevant for designing systems with specific energy transfer characteristics, where controlling the number of states or particles could tailor the transition probabilities. This analysis is crucial for applications in quantum optics, photonics, and condensed matter physics, where precise control over energy transfer is often required. This work contributes to the ongoing research on photon and quasiparticle dynamics in quantum systems by providing a detailed numerical analysis of transition rates within a cavity. The observed effects of varying n align well with previous findings in the field, particularly regarding the relationship between transition rates, energy gaps, and the density of available states. By comparing our results with earlier studies in cavity QED, superconducting circuits, low-dimensional systems, and nanostructures, we have highlighted the broader relevance of our findings and reinforced the importance of controlling state availability and energy gaps in designing quantum systems with tailored transition characteristics. This study advances the understanding of quasiparticle-photon dynamics in quantum systems by offering a more detailed examination of the transition rates for photon-quasiparticle emission within a cavity. Compared to previous works, such as those by Blais et al. [9] and Viitanen et al. [2], which focused on cQED and quasiparticle tunneling, this research specifically quantifies how transition rates vary with energy gaps, photon frequencies, and temperature, providing insights into the interaction between photons and quasiparticles. By studying both the normalized superconductor quasiparticle density states and the effective T_{QCR}, this work contributes a nuanced understanding of the photon-assisted tunneling dynamics, particularly how these factors impact coherence times and the efficiency of quantum systems. The findings have practical implications for optimizing quantum computing operations such as qubit initialization and readout, thereby improving overall system performance.

As the inverse temperature β increases, corresponding to a decrease in temperature, the transition rate $F(E)$ decreases for all values of n as shown in Figure 3. This inverse relationship between β and $F(E)$ is expected and aligns with fundamental principles of quantum mechanics and statistical physics. At lower temperatures (higher β), the thermal excitation of particles is reduced, leading to fewer transitions between energy states. This reduction in thermal excitation diminishes the likelihood of photons or quasiparticles transitioning from the cavity, hence the observed decrease in $F(E)$. This trend can be understood through the Boltzmann distribution, where the probability of a system occupying a higher energy state decreases exponentially with temperature. In systems where quantum effects dominate, such as in cavity QED or quantum dots, this temperature dependency is crucial for determining the transition dynamics.

The parameter n represents a system-specific factor that could relate to the number of particles, the strength of coupling in the system, or other quantum mechanical properties. For $n = 1$, the transition rate $F(E)$ is generally lower across the entire β range. This suggests that the system has a lower capacity for transitions at this smaller n value, likely due to weaker coupling or fewer available states for transitions. As n increases to 10 and 50, the transition rate increases significantly, and the curves shift

Figure 3
Transition rate of photon-quasiparticles through cavity with temperature

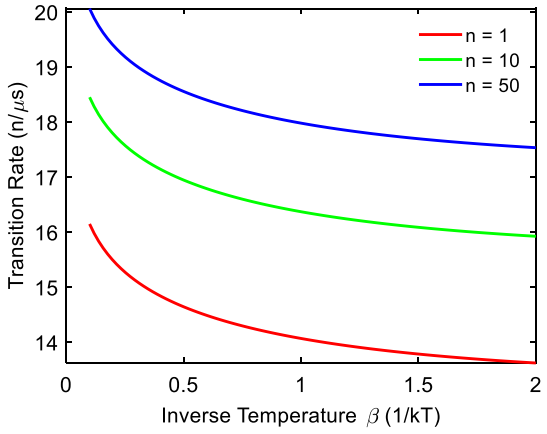

upwards. This upward shift indicates that a higher n value enhances the system's transition capacity. This could be due to stronger coupling in the system or a greater number of accessible states, which increases the probability of transitions occurring.

In studies involving cavity QED, the transition rates have been observed to decrease with lowering temperature due to reduced thermal excitations. This aligns with the trend seen in the current graph, where $F(E)$ decreases as β increases (temperature decreases). The increase in transition rates with higher n values mirrors the results in quantum dot and superconducting circuit studies, where the size of the system or the strength of coupling plays a significant role in determining transition rates. For instance, in superconducting qubits, the coupling strength between the qubit and the cavity field directly affects the transition rates, similar to the observed influence of n in the current graph. This analysis highlights the critical role that temperature and system-specific parameters (like n) play in governing the behavior of transitions in confined quantum systems. The observed trends and comparisons with previous work provide valuable insights into the quantum mechanical principles underlying these transitions, reaffirming the established theoretical frameworks.

The graph illustrates the relationship between the energy difference E and the transition rate $F(E)$ in a quantum system as shown in Figure 4. The peak observed in the graph can be associated with a resonant energy level where the transition rate is maximized. This resonates with the concept of quantum transitions where particles (e.g., electrons) are more likely to transition between energy states when the energy difference E aligns with certain system-specific parameters, such as the Fermi energy E_f. The inverse temperature parameter β influences the shape of the curve, particularly in the regions close to E_f. A higher β (lower temperature) tends to sharpen the transition, concentrating the transitions around the resonant energy, while a lower β (higher temperature) would broaden the distribution, allowing transitions over a wider range of energy differences. The

Figure 4
Transition rate at (a) $\beta = 1$, (b) $\beta = 10$, (c) $\beta = 50$, and (d) $\beta = 100$ with energy gap of superconductors

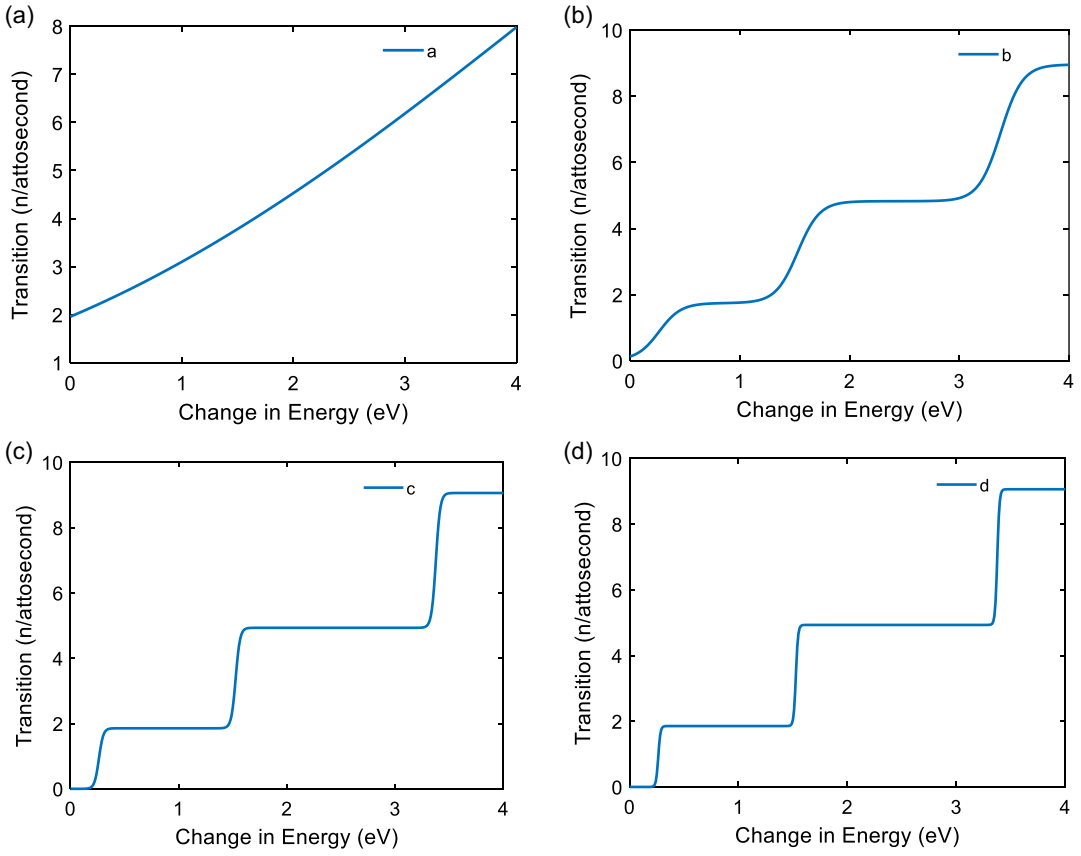

factor γ_D introduces a broadening to the resonant peak, reflecting the lifetime of the excited states. A smaller γ_D would result in a sharper peak, indicative of less dissipation in the system, whereas a larger γ_D would broaden the peak, indicating stronger damping effects.

A linear increase in transition rate with energy suggests that the system's probability of transitioning between states rises steadily with energy. This linear trend may indicate that, at this temperature, the system is in a regime where energy levels contribute progressively and uniformly to the transition rate. Essentially, as energy increases, more states become available for transitions, leading to a proportional increase in the transition rate. At $\beta = 1$ (a moderate temperature), the thermal distribution of particles follows a simpler pattern where transitions are uniformly distributed over the range of energies. This suggests a relatively stable thermal environment with moderate excitation levels, where the energy distribution affects transitions in a straightforward manner.

The wave-like behavior reflects the influence of temperature on the transition rate. At higher β (lower temperature), the thermal distribution becomes sharper, leading to more pronounced oscillations in the transition probability. This is because, at lower temperatures, the occupation probabilities of quantum states become more sensitive to energy changes, resulting in periodic variations in the transition rate. The wave-like pattern suggests that at $\beta = 2$, the system experiences distinct resonant conditions where transitions are more probable at specific energy intervals. This behavior indicates a stronger influence of discrete energy levels and their corresponding occupation probabilities, characteristic of lower temperature regimes where thermal broadening is reduced, and energy differences become more pronounced.

For $\beta > 2$, the transition rate shows a stair-step or piecewise linear behavior shown in Figure 4(c) and (d). The stair-step pattern indicates that the transition rate increases in discrete steps rather than continuously. This can be attributed to the increasingly sharp and well-defined energy states at lower temperatures. The system now exhibits distinct energy thresholds or quantization effects where transitions occur more readily at certain energy levels, and the rate remains relatively constant between these thresholds. At higher β values (lower temperatures), the thermal distribution of particles becomes very narrow around the Fermi energy. As a result, transitions are more discrete, and the system behaves in a piecewise manner where the transition rate jumps between different energy levels rather than varying smoothly. This reflects a low-temperature regime where only specific energy differences contribute significantly to transitions due to the highly quantized nature of the energy states. The parameter β increases (which corresponds to a decrease in temperature), more particles are found in distinct energy density states within the cavity. This results in a stepwise transition pattern, similar to stair steps, where each step represents a higher probability of photon-quasiparticle interactions. The larger the steps, the greater the likelihood of a significant number of photon-quasiparticle transitions occurring. This implies that at lower temperatures, the system exhibits more pronounced, quantized transitions, reflecting the increased stability and interaction strength between photons and quasiparticles in the cavity.

As β increases, the transition rate $F(E)$ generally increases as shown in Figure 5. This trend aligns with the physical expectation that lower temperatures reduce thermal excitation and hence the transition probability. For a fixed β, the transition rate for $\chi_n = 1$ is higher than for $\chi_n = 10$. This suggests that a lower χ_n (which corresponds to a lower photon number) results in a stronger

Figure 5
Transition rate at $\chi_n = 1$, $\chi_n = 5$, and $\chi_n = 10$ with temperature

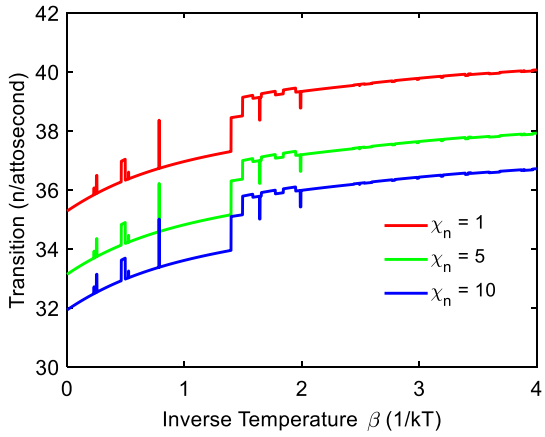

effective coupling, leading to a higher transition rate. As χ_n increases, the effective coupling decreases due to the increased cavity pull, thus reducing the transition rate. The graph shows fluctuations in the lower region of β, with both up and down peaks observed. These fluctuations are more pronounced for lower χ_n values and become less significant as χ_n increases. The presence of peaks and valleys below $\beta = 2$ indicates that, at higher temperatures (lower β), the transition rate is sensitive to changes in energy, and the effect of thermal excitation becomes more noticeable. These fluctuations can be attributed to the interplay between thermal effects and the energy-dependent transition rates. At higher temperatures (lower β), the population of excited states increases, leading to more complex interactions that can cause oscillatory behavior in the transition rates. The sensitivity of the transition rate to energy changes is more evident in this regime, as indicated by the observed peaks and valleys as shown in Figure 5.

The observed decrease in transition rate with increasing β (decreasing temperature) is consistent with previous studies in quantum systems, such as those involving cavity QED and quantum dots. Lower temperatures generally reduce thermal excitations, leading to lower transition rates. The comparison between $\chi_n = 1$ and $\chi_n = 10$ aligns with theoretical expectations where a lower photon number (and hence a lower cavity pulls effect) results in a higher transition rate as shown in Figure 4. This mirrors findings from studies on quantum systems where coupling strength and system parameters significantly affect transition dynamics. The observed fluctuations at lower β are similar to phenomena reported in systems with complex thermal excitation dynamics. In quantum systems, such as superconducting circuits and quantum dots, similar temperature-dependent behaviors have been observed, where thermal excitation causes oscillatory effects in transition rates. The increasing and decreasing toothpick valley-like nature in Figure 5 is due to interference between photon-quasiparticles within the cavity of system.

The graph shows in Figure 6 the temperature T_{QCR} as a function of the energy gap, which spans from −2 eV to 2 eV. The temperature T_{QCR} is calculated using the mean photon number relation and the formula Equation (6) for the effective temperature of the QCR environment. As the energy gap eV changes, the temperature T_{QCR} exhibits a non-linear behavior. Specifically, the temperature values show significant variations depending on whether eV is

positive or negative. The temperature T_{QCR} generally increases with the magnitude of the energy gap eV. This indicates that larger energy gaps correspond to higher effective temperatures in the QCR environment. At larger positive energy gaps, T_{QCR} tends to decrease, showing that for high energy gaps, the system behaves as if it is at a lower effective temperature. For larger negative energy gaps, the temperature T_{QCR} increases, indicating that the effective temperature of the QCR environment increases with decreasing energy gaps.

The variation of T_{QCR} with eV reflects how the effective temperature of the QCR environment is influenced by the energy gap in Figure 6. This is consistent with the theoretical understanding that the population of states with the energy gap, affecting the effective temperature. The expression for T_{QCR} involves the ratio, which is related to the photon number in the cavity. The changes in T_{QCR} with eV reveal how the mean photon number and the coupling environment affect the thermal state of the system. For different energy gaps, the relative populations and the effective temperature vary, showing the complex interplay between these factors. The graph indicates that the temperature of the QCR environment is sensitive to changes in the energy gap. This sensitivity is essential for understanding the thermal behavior of quantum systems and the dynamics of photon interactions within the cavity.

As β increases, the temperature T_{QCR} generally decreases as shown in Figure 7. This is because a higher β (or lower temperature) typically reduces the thermal excitation effects, leading to a lower effective temperature in the QCR system. For $\omega_r = 1$ eV, the T_{QCR} values are relatively higher compared to the other photon frequencies. This suggests that for lower photon frequencies, the system's effective temperature is higher for the same inverse temperature. For $\omega_r = 5$ eV and $\omega_r = 10$ eV, As ω_r increases, the T_{QCR} decreases more rapidly with increasing β. Higher photon frequencies lead to a more pronounced effect of the inverse temperature on the effective temperature. At lower values of β, the curves tend to show higher temperatures. This aligns with the expectation that at higher temperatures (low β), the system's effective temperature is less sensitive to the photon frequency. As β increases, T_{QCR} decreases more steeply for higher ω_r values. This indicates that the system's effective temperature becomes more sensitive to changes in β when the photon frequency is higher.

Figure 6
Effective temperature with energy gap inside quantum cavity

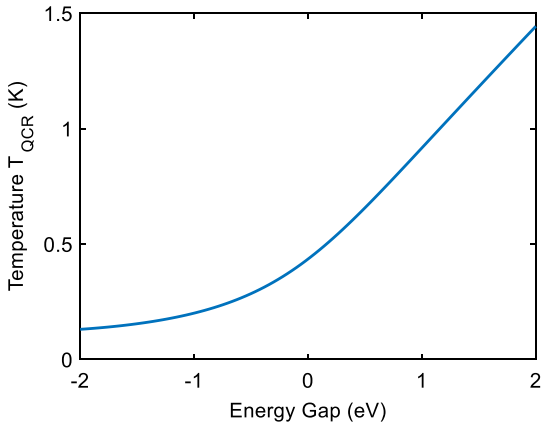

Figure 7
Effective temperature with temperature at different energy of photon-quasiparticle

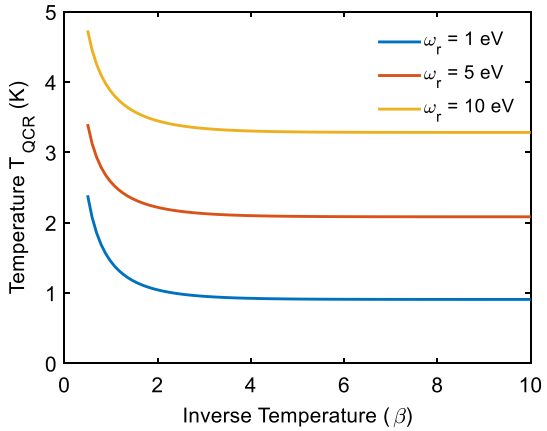

The effective temperature T_{QCR} derived from the photon number and energy gap reflects the thermal dynamics of the system. The decrease in T_{QCR} with increasing β is consistent with the theoretical understanding that lower temperatures lead to reduced excitation effects. Higher photon frequencies ω_r result in a more significant decrease in T_{QCR} with increasing β. This indicates that the thermal properties of the system become more sensitive to changes in the photon frequency at lower temperatures. This behavior is relevant in various quantum systems where photon interactions and thermal states play crucial roles, such as in cavity QED and quantum optical systems. The graph provides insights into how photon frequency and temperature affect the thermal properties of these systems. The results align with theoretical predictions that the effective temperature of a thermal resonator or quantum system is influenced by both the energy gap and the photon frequency. The observed trends are consistent with the expected behavior of such systems under varying thermal and photon conditions.

4. Conclusion

The analysis of photon and quasiparticle transition rates within a cavity demonstrates a clear dependency on both the energy gap and the number of photon-quasiparticles, which represents the number of particles or states. For smaller values of n, the transition rates are more localized around the Fermi energy, reflecting a higher probability of transitions due to a reduced number of available states. As n increases, the transition rates become more dispersed, indicating a broader distribution of states and a decrease in the peak transition probability. The inverse temperature β plays a crucial role in modulating the transition rates, with higher temperatures (lower β) leading to increased transition rates due to enhanced thermal excitation. Conversely, higher β values result in lower transition rates as thermal excitation diminishes. The effective temperature T_{QCR} of the cavity is sensitive to changes in both the energy gap and the photon frequency ω_r, with T_{QCR} generally increasing with the energy gap and decreasing with higher photon frequencies. These findings offer valuable insights into the dynamics of photon and quasiparticle transitions in quantum systems. The observed effects of varying n and β align with theoretical expectations and provide a deeper understanding of the interplay between temperature, energy gaps, and state

distributions in quantum systems. The results have significant implications for the design and optimization of systems in quantum optics, photonics, and condensed matter physics, where precise control over energy transfer and transition probabilities is crucial.

Ethical Statement

This study does not contain any studies with human or animal subjects performed by any of the authors.

Conflicts of Interest

The authors declare that they have no conflicts of interest to this work.

Data Availability Statement

Data are available from the corresponding author upon reasonable request.

Author Contribution Statement

Jayanti Chand: Conceptualization, Methodology, Software, Formal analysis, Resources, Data curation, Writing – original draft, Writing – review & editing, Visualization. **Kishori Yadav:** Software, Validation, Investigation, Supervision, Project administration. **Saddam Husain Dhobi:** Conceptualization, Methodology, Software, Validation, Formal analysis, Investigation, Resources, Data curation, Writing – original draft, Writing – review & editing, Visualization, Supervision, Project administration.

References

[1] Ullah, A., Tahir Naseem, M., & Müstecaplıoğlu, Ö. E. (2024). Mixing thermal coherent states for precision and range enhancement in quantum thermometry. *Quantum Science and Technology, 10*(1), 015044. https://doi.org/10.1088/2058-9565/ad994a

[2] Viitanen, A., Mörstedt, T., Teixeira, W. S., Tiiri, M., Räbinä, J., Silveri, M., & Möttönen, M. (2024). Quantum-circuit refrigeration of a superconducting microwave resonator well below a single quantum. *Physical Review Research, 6*(2), 023262. https://doi.org/10.1103/PhysRevResearch.6.023262

[3] Tabatabaei, S. M., & Jahangiri, N. (2024). Quantum circuit refrigerator based on quantum dots coupled to normal-metal and superconducting electrodes. *Physical Review B, 110*(4), 045433. https://doi.org/10.1103/PhysRevB.110.045433

[4] Krasnok, A., Dhakal, P., Fedorov, A., Frigola, P., Kelly, M., & Kutsaev, S. (2024). Superconducting microwave cavities and qubits for quantum information systems. *Applied Physics Reviews, 11*(1), 011302. https://doi.org/10.1063/5.0155213

[5] Connolly, T., Kurilovich, P. D., Diamond, S., Nho, H., Bøttcher, C. G. L., Glazman, L. I., . . . , & Devoret, M. H. (2024). Coexistence of nonequilibrium density and equilibrium energy distribution of quasiparticles in a superconducting qubit. *Physical Review Letters, 132*(21), 217001. https://doi.org/10.1103/PhysRevLett.132.217001

[6] Cheng, J., Zuo, X., Wang, J., & Xing, Y. (2024). Quasiparticle trapping in quench dynamics of superconductor/quantum dot/superconductor Josephson junctions. *Physical Review B, 110*(12), 125417. https://doi.org/10.1103/PhysRevB.110.125417

[7] Dubovitskii, K. S., Basko, D. M., Meyer, J. S., & Houzet, M. (2024). Theory of quasiparticle-induced errors in driven-dissipative Schrödinger cat qubits. *Physical Review B, 110*(2), 024505. https://doi.org/10.1103/PhysRevB.110.024505

[8] Pita-Vidal, M., Wesdorp, J. J., Splitthoff, L. J., Bargerbos, A., Liu, Y., Kouwenhoven, L. P., & Andersen, C. K. (2024). Strong tunable coupling between two distant superconducting spin qubits. *Nature Physics, 20*(7), 1158–1163. https://doi.org/10.1038/s41567-024-02497-x

[9] Blais, A., Grimsmo, A. L., Girvin, S. M., & Wallraff, A. (2021). Circuit quantum electrodynamics. *Reviews of Modern Physics, 93*(2), 025005. https://doi.org/10.1103/RevModPhys.93.025005

[10] Kjaergaard, M., Schwartz, M. E., Braumüller, J., Krantz, P., Wang, J. I.-J., Gustavsson, S., & Oliver, W. D. (2020). Superconducting qubits: Current state of play. *Annual Review of Condensed Matter Physics, 11*, 369–395. https://doi.org/10.1146/annurev-conmatphys-031119-050605

[11] Kim, Y., Eddins, A., Anand, S., Wei, K. X., van den Berg, E., Rosenblatt, S., . . . , & Kandala, A. (2023). Evidence for the utility of quantum computing before fault tolerance. *Nature, 618*(7965), 500–505. https://doi.org/10.1038/s41586-023-06096-3

[12] Harrington, P. M., Mueller, E. J., & Murch, K. W. (2022). Engineered dissipation for quantum information science. *Nature Reviews Physics, 4*(10), 660–671. https://doi.org/10.1038/s42254-022-00494-8

[13] Yoshioka, T., Mukai, H., Tomonaga, A., Takada, S., Okazaki, Y., Kaneko, N.-H., . . . , & Tsai, J.-S. (2023). Active initialization experiment of a superconducting qubit using a quantum circuit refrigerator. *Physical Review Applied, 20*(4), 044077. https://doi.org/10.1103/PhysRevApplied.20.044077

[14] Pietikäinen, I., Černotík, O., Eickbusch, A., Maiti, A., Garmon, J. W. O., Filip, R., & Girvin, S. M. (2024). Strategies and trade-offs for controllability and memory time of ultra-high-quality microwave cavities in circuit quantum electrodynamics. *PRX Quantum, 5*(4), 040307. https://doi.org/10.1103/PRXQuantum.5.040307

[15] Yoshioka, T., & Tsai, J. S. (2021). Fast unconditional initialization for superconducting qubit and resonator using quantum-circuit refrigerator. *Applied Physics Letters, 119*(12), 124003. https://doi.org/10.1063/5.0057894

[16] Sevriuk, V. A., Liu, W., Rönkkö, J., Hsu, H., Marxer, F., Mörstedt, T. F., . . . , & Möttönen, M. (2022). Initial experimental results on a superconducting-qubit reset based on photon-assisted quasiparticle tunneling. *Applied Physics Letters, 121*(23), 234002. https://doi.org/10.1063/5.0129345

[17] Maclay, G. J. (2020). History and some aspects of the Lamb shift. *Physics, 2*(2), 105–149. https://doi.org/10.3390/physics2020008

[18] Hatridge, M., Shankar, S., Mirrahimi, M., Schackert, F., Geerlings, K., Brecht, T., . . . , & Devoret, M. H. (2013). Quantum back-action of an individual variable-strength measurement. *Science, 339*(6116), 178–181. https://doi.org/10.1126/science.1226897

[19] Mabuchi, H., & Doherty, A. C. (2002). Cavity quantum electrodynamics: Coherence in context. *Science, 298*(5597), 1372–1377. https://doi.org/10.1126/science.1078446

[20] Ulbricht, G., de Lucia, M., & Baldwin, E. (2021). Applications for Microwave Kinetic Induction Detectors in advanced instrumentation. *Applied Sciences, 11*(6), 2671. https://doi.org/10.3390/app11062671

[21] Mandal, K. K., Singh, A. K., Kumar, B., Shah, A. P., Vij, R., Majumder, A., . . . , & Kumar, A. (2024). Emission engineering in monolithically integrated silicon nitride microring resonators. *ACS Materials Letters, 6*(5), 1831–1840. https://doi.org/10.1021/acsmaterialslett.4c00105

[22] Hofheinz, M., Wang, H., Ansmann, M., Bialczak, R. C., Lucero, E., Neeley, M., . . . , & Cleland, A. N. (2009). Synthesizing arbitrary quantum states in a superconducting resonator. *Nature, 459*(7246), 546–549. https://doi.org/10.1038/nature08005

[23] Elshaari, A. W., Pernice, W., Srinivasan, K., Benson, O., & Zwiller, V. (2020). Hybrid integrated quantum photonic circuits. *Nature Photonics, 14*(5), 285–298. https://doi.org/10.1038/s41566-020-0609-x

[24] Gusenkova, D., Spiecker, M., Gebauer, R., Willsch, M., Willsch, D., Valenti, F., . . . , & Pop, I. M. (2021). Quantum nondemolition dispersive readout of a superconducting artificial atom using large photon numbers. *Physical Review Applied, 15*(6), 064030. https://doi.org/10.1103/PhysRevApplied.15.064030

[25] Hanai, R., McDonald, A., & Clerk, A. (2021). Intrinsic mechanisms for drive-dependent Purcell decay in superconducting quantum circuits. *Physical Review Research, 3*(4), 043228. https://doi.org/10.1103/PhysRevResearch.3.043228

[26] Khezri, M., Opremcak, A., Chen, Z., Miao, K. C., McEwen, M., Bengtsson, A., . . . , & Smelyanskiy, V. (2023). Measurement-induced state transitions in a superconducting qubit: Within the rotating-wave approximation. *Physical Review Applied, 20*(5), 054008. https://doi.org/10.1103/PhysRevApplied.20.054008

[27] Janvier, C., Tosi, L., Bretheau, L., Girit, Ç. Ö., Stern, M., Bertet, P., . . . , & Urbina, C. (2015). Coherent manipulation of Andreev states in superconducting atomic contacts. *Science, 349*(6253), 1199–1202. https://doi.org/10.1126/science.aab2179

[28] Beenakker, C. W. J., & van Houten, H. (1991). Josephson current through a superconducting quantum point contact shorter than the coherence length. *Physical Review Letters, 66*(23), 3056–3059. https://doi.org/10.1103/PhysRevLett.66.3056

[29] Das, S. K., Dhobi, S. H., & Nakarmi, J. J. (2022). 2D electron system with quasiparticle auxiliary field correlation of open quantum system. *Patan Prospective Journal, 2*(1), 176–187. https://doi.org/10.3126/ppj.v2i1.48135

[30] Abdurakhimov, L. V., Mahboob, I., Toida, H., Kakuyanagi, K., Matsuzaki, Y., & Saito, S. (2022). Identification of different types of high-frequency defects in superconducting qubits. *PRX Quantum, 3*(4), 040332. https://doi.org/10.1103/PRXQuantum.3.040332

[31] Schiela, W. F., Yu, P., & Shabani, J. (2024). Progress in super conductor-semiconductor topological Josephson junctions. *PRX Quantum, 5*(3), 030102. https://doi.org/10.1103/PRXQuantum.5.030102

[32] Rauschenbeutel, A., Nogues, G., Osnaghi, S., Bertet, P., Brune, M., Raimond, J. M., & Haroche, S. (2000). Step-by-step engineered multiparticle entanglement. *Science, 288*(5473), 2024–2028. https://doi.org/10.1126/science.288.5473.2024

[33] Hood, C. J., Lynn, T. W., Doherty, A. C., Parkins, A. S., & Kimble, H. J. (2000). The atom-cavity microscope: Single atoms bound in orbit by single photons. *Science, 287*(5457), 1447–1453. https://doi.org/10.1126/science.287.5457.1447

[34] Karimi, B., Chang, Y.-C., & Pekola, J. P. (2022). Low temperature characteristics of the metal-Superconductor NIS tunneling thermometer. *Journal of Low Temperature Physics, 207*(3), 220–225. https://doi.org/10.1007/s10909-022-02713-z

[35] Dynes, R. C., Narayanamurti, V., & Garno, J. P. (1978). Direct measurement of quasiparticle-lifetime broadening in a strong-coupled superconductor. *Physical Review Letters, 41*(21), 1509–1512. https://doi.org/10.1103/PhysRevLett.41.1509

How to Cite: Chand, J., Yadav, K., & Dhobi, S. H. (2025). Quasiparticle-Photon Transitions in Superconductors Within a QED Cavity. *Journal of Optics and Photonics Research*, *3*(1), 1–10. https://doi.org/10.47852/bonviewJOPR52024257